Optimal multifilter banks: Design, related symmetric extension transform and application to image compression

Tao Xia† and Qingtang Jiang‡

Abstract— **The design of optimal multifilter banks and optimum time–frequency resolution multiwavelets with different objective functions is discussed. The symmetric extension transform related to multifilter banks with the symmetric properties is presented. It is shown that such a symmetric extension transform is nonexpansive. More optimal multifilter banks for image compression are constructed and some of them are used in image compression. Experiments show that optimal multifilter banks have better performances in image compression than Daubechies' orthogonal wavelet filters and Daubechies' least asymmetric wavelet filters, and for some images, they even have better performances than the scalar $(9, 7)$–tap biorthogonal wavelet filters. Experiments also show that the symmetric extension transform provided in this paper improves the rate–distortion performance, compared with the periodic extension transform.**

EDICS No: SP 2.4.4.
Keywords— **Balanced multiwavelet, discrete multiwavelet transform, image compression, multifilter bank, multiwavelet, nonexpansive symmetric extension transform, symmetry, time–frequency resolution.**

I. Introduction

Multiwavelets, wavelets generated by a finite set of scaling functions, have several advantages in comparison to scalar wavelets (see [18]). One of the advantages is that a multiwavelet can possess the orthogonality and symmetry simultaneously, while except for the Haar system, a scalar wavelet can not have these two properties at the same time ([4] and [17]). Thus, as stated in [18], multiwavelets offer the possibility of superior performance for image processing applications, compared with the scalar wavelets. As it was shown in [18], the DGHM multiwavelet, which was constructed by Donovan, Geronimo, Hardin and Massopust in [5] and [7], has a good performance in signal denoising. However for image compression, the DGHM multiwavelet does not have a good performance as one expected [18], and more multiwavelets which are more suitable for image compression are desired. In [11], the construction of optimum time–frequency resolution (**OPTFR**) multiwavelets was proposed and the optimal multiwavelet filter banks suitable for image compression were designed in [12]. In this paper, we discuss the design of OPTFR multiwavelets with different objective functions and provide more optimal multiwavelet filter banks. The constructed optimal multiwavelet filter banks have the symmetric properties. For symmetric multiwavelet filter banks, a symmetric extension transform of the finite–length input signals is desired. This paper provides such a symmetric extension transform and proves that the symmetric extension transform is nonexpansive. Based on the symmetric extension transform, we use optimal multiwavelet filter banks in image compression. Experiments show that OPTFR multiwavelets have better performances in image compression than Daubechies' orthogonal wavelets and Daubechies' least asymmetric wavelets, and for some images, OPTFR multiwavelets even have better performance than the scalar $(9, 7)$–tap biorthogonal wavelet.

This paper is organized as follows. In Section 2, we review the definition of multiwavelets, the discrete multiwavelet transform, and the procedure to construct OPTFR multiwavelets. In Section 3, we develop the nonexpansive symmetric extension transform for multiwavelet filter banks with the symmetric property. In Section 4, first we discuss the objective functions for the construction of OPTFR multiwavelets for image compression, then we give the implementation of OPTFR multiwavelets for image compression and provide the image compression results with scalar wavelets and OPTFR multiwavelets. The conclusions are given in Sections 5.

II. Multifilter banks and multiwavelets

In this section, we review the definitions of multiwavelet filter banks and multiwavelets, the discrete multiwavelet transform and the procedure to construct OPTFR multiwavelets.

A. Discrete multiwavelet transform

A vector-valued function $\Psi := (\psi_1, \cdots, \psi_r)^T$ is called a multiwavelet if the collections of the integer translates and the dilations of factor 2 of $\psi_1, \cdots, \psi_r$ form an orthonormal basis of $L^2(R)$. To construct a compactly supported multiwavelet, we begin with two $r \times r$ matrices $\mathbf{H}(\omega) = \sum_{k\in Z} \mathbf{H}_k e^{-ik\omega}$ and $\mathbf{G}(\omega) = \sum_{k\in Z} \mathbf{G}_k e^{-ik\omega}$ of

Manuscript received Feb., 1998. The associate editor coordinating the review of this paper and approving it for publication was Dr. Hitoshi Kiya
†Supported by an NSTB post-doctoral research fellowship at National University of Singapore.
‡Supported by the Wavelets Strategic Research Programme, National University of Singapore, under a grant from NSTB and the Ministry of Education, Singapore.
The authors are with the Department of Mathematics, National University of Singapore, Singapore 119260 (E-mail: xiatao@haar.math.nus.edu.sg, qjiang@haar.math.nus.edu.sg).

trigonometric polynomials satisfying

$$\begin{cases} \mathbf{H}(\omega)\mathbf{H}^*(\omega) + \mathbf{H}(\omega+\pi)\mathbf{H}^*(\omega+\pi) = \mathbf{I}_r, \\ \mathbf{H}(\omega)\mathbf{G}^*(\omega) + \mathbf{H}(\omega+\pi)\mathbf{G}^*(\omega+\pi) = \mathbf{0}_r, \\ \mathbf{G}(\omega)\mathbf{G}^*(\omega) + \mathbf{G}(\omega+\pi)\mathbf{G}^*(\omega+\pi) = \mathbf{I}_r, \end{cases} \tag{1}$$

where $-\pi < \omega \le \pi$. Throughout this paper, $\mathbf{B}^*$ denotes the Hermitian adjoint of the matrix $\mathbf{B}$, and $\mathbf{I}_r$ and $\mathbf{0}_r$ denote the $r \times r$ identity matrix and zero matrix respectively. If the transition operator $\mathcal{T}_{\mathbf{H}}$ associated with $\mathbf{H}$ satisfies Condition E (A matrix $\mathbf{D}$ is said to satisfy **Condition E** if 1 is a simple eigenvalue of $\mathbf{D}$ and all other eigenvalues lie inside the open unit disk), then there exists a unique compactly supported solution Φ with $\widehat{\Phi}(0) \neq 0$ of the refinement equation

$$\Phi(x) = 2\sum_{k\in Z} \mathbf{H}_k \Phi(2x-k). \tag{2}$$

Furthermore Φ is a scaling function, i.e., Φ generates a multiresolution analysis of multiplicity r, and Ψ defined by

$$\Psi(x) = 2\sum_{k\in Z} \mathbf{G}_k \Phi(2x-k), \tag{3}$$

is a multiwavelet, see e.g., [12]. In this case we say that $\{\mathbf{H},\mathbf{G}\}$ generates the scaling function Φ and the multiwavelet Ψ. The pair $\{\mathbf{H},\mathbf{G}\}$ is called a multiwavelet filter bank (this is often abbreviated **multifilter bank**), and $\mathbf{H}$ ($\mathbf{G}$, respectively) is called a **matrix lowpass filter** (**matrix highpass filter**, respectively). For a multifilter bank $\{\mathbf{H},\mathbf{G}\}$, it is said to be a **finite impulse response (FIR)** multifilter bank if there exists an integer N such that $\mathbf{H}_k = \mathbf{0}, \mathbf{G}_k = \mathbf{0}, |k| > N$. A multifilter bank $\{\mathbf{H},\mathbf{G}\}$ is said to be orthogonal if it satisfies (1). In this paper, scaling functions, multiwavelets, and the filter coefficients of the multifilter banks discussed are real.

Assume that $\{\mathbf{H},\mathbf{G}\}$ is an orthogonal FIR multifilter bank and it generates a compactly supported scaling function $\Phi = (\phi_1,\cdots,\phi_r)^T$ and a multiwavelet $\Psi = (\psi_1,\cdots,\psi_r)^T$. Let (V_j) be the multiresolution analysis generated by Φ, i.e., $V_j = \overline{\text{span}}\{\phi_\ell(2^j\cdot -k), 1\le \ell \le r, k\in Z\}$. Denote $W_j := V_{j+1} \ominus V_j, j \in Z$, the orthogonal complement of V_j in V_{j+1}. Then $\{2^{\frac{j}{2}}\phi_\ell(2^j\cdot -k)\}_{1\le\ell\le r,k\in Z}$ and $\{2^{\frac{j}{2}}\psi_\ell(2^j\cdot -k)\}_{1\le\ell\le r,k\in Z}$ are orthonormal bases of V_j and W_j, $j\in Z$, respectively. For any continuous function $f(t)$ in V_0, it can be expanded as

$$f(t) = \sum_n \sum_{\ell=1}^r c_{\ell,n}^{(0)} \phi_\ell(t-n).$$

The function f is completely determined by the sequence $\{(c_{1,n}^{(0)},\cdots,c_{r,n}^{(0)})^T\}$. Let J be a negative integer. By the fact $V_0 = W_{-1}\oplus V_{-1} = \cdots = W_{-1}\oplus\cdots\oplus W_J \oplus V_J$, and the orthonormality of $2^{\frac{j}{2}}\phi_\ell(2^j\cdot -k)$ and $2^{\frac{j}{2}}\psi_\ell(2^j\cdot -k)$, f also can be expanded as

$$\begin{aligned} f(t) &= \sum_n\sum_{\ell=1}^r c_{\ell,n}^{(-1)}\frac{1}{\sqrt{2}}\phi_\ell(\frac{t}{2}-n) \\ &\quad + \sum_n\sum_{\ell=1}^r d_{\ell,n}^{(-1)}\frac{1}{\sqrt{2}}\psi_\ell(\frac{t}{2}-n) \\ &= \cdots \\ &= \sum_n\sum_{\ell=1}^r c_{\ell,n}^{(J)} 2^{\frac{J}{2}}\phi_\ell(2^J t-n) \\ &\quad + \sum_{j=J}^{-1}\sum_n\sum_{\ell=1}^r d_{\ell,n}^{(j)} 2^{\frac{j}{2}}\psi_\ell(2^j t-n), \end{aligned}$$

where $c_{\ell,n}^{(j)}, d_{\ell,n}^{(j)} \in R$ are given by

$$c_{\ell,n}^{(j)} = \int f(t)2^{\frac{j}{2}}\phi_\ell(2^j t-k)dt,$$
$$d_{\ell,n}^{(j)} = \int f(t)2^{\frac{j}{2}}\psi_\ell(2^j t-k)dt.$$

Denote $\mathbf{c}_n^{(j)} := (c_{1,n}^{(j)},\cdots,c_{r,n}^{(j)})^T$, $\mathbf{d}_n^{(j)} := (d_{1,n}^{(j)},\cdots,d_{r,n}^{(j)})^T$. Then we have

$$\begin{aligned} &\sum_n (\mathbf{c}_n^{(j)})^T 2^{\frac{j}{2}}\Phi(2^j t-n) \\ &= \sum_n (\mathbf{c}_n^{(j-1)})^T 2^{\frac{j-1}{2}}\Phi(2^{j-1}t-n) \\ &\quad + \sum_n (\mathbf{d}_n^{(j-1)})^T 2^{\frac{j-1}{2}}\Psi(2^{j-1}t-n). \end{aligned} \tag{4}$$

Multiplying both sides of (4) with $2^{\frac{j-1}{2}}\Phi(2^{j-1}t-k)^T$ and taking integral over R, we have

$$\mathbf{c}_k^{(j-1)} = \sqrt{2}\sum_n \mathbf{H}_{n-2k}\mathbf{c}_n^{(j)}. \tag{5}$$

Similarly by multiplying both sides of (4) with $2^{\frac{j-1}{2}}\Psi(2^{j-1}t-k)^T$ and taking integral over R, one has

$$\mathbf{d}_k^{(j-1)} = \sqrt{2}\sum_n \mathbf{G}_{n-2k}\mathbf{c}_n^{(j)}. \tag{6}$$

Finally, multiply both sides of (4) with $2^{\frac{j}{2}}\Phi(2^j t-k)^T$ and take integral over R, we have

$$\mathbf{c}_k^{(j)} = \sqrt{2}\sum_n \mathbf{H}_{k-2n}^T\mathbf{c}_n^{(j-1)} + \sqrt{2}\sum_n \mathbf{G}_{k-2n}^T\mathbf{d}_n^{(j-1)}. \tag{7}$$

Equations (5) and (6) are the discrete multiwavelet transform decomposition algorithm, while (7) is the reconstruction algorithm (see also [18] and [22]). Thus to determine $\mathbf{c}_k^{(J)}$ and $\mathbf{d}_n^{(j-1)}$, $J\le j\le -1$, we need only to determine $\mathbf{c}_n^{(0)}$ from $f(t)$.

For the scalar wavelet transform, since the scaling function ϕ satisfies $\widehat{\phi}(0) = 1$, $c_n^{(0)}$ is close to $f(n/N_0)$ and we simply let $c_n^{(0)}$ to be $f(n/N_0)$, where $f(n/N_0)$ are samples of $f(t)$ with sampling rate $1/N_0$. However for the multiwavelet transform, $\widehat{\Phi}(0)$ is a normalized right 1-eigenvector of $\mathbf{H}(0)$ (see [12]), and $\widehat{\Phi}(0)$ needs not have to be $\frac{1}{\sqrt{r}}(1,\cdots,1)^T$. In this case, we can not simply determine $\mathbf{c}_n^{(0)}$ in such a way as in the scalar case. There are two methods to deal with this problem. One method is the pre/postfilter techniques carried out in [18], [21] and [22]. Another method is to use another pair of multifilter bank $\{\mathbf{H}^b, \mathbf{G}^b\}$ constructed from $\{\mathbf{H}, \mathbf{G}\}$. This new multifilter bank $\{\mathbf{H}^b, \mathbf{G}^b\}$ generates the scaling function Φ^b and multiwavelet Ψ^b with $\widehat{\Phi}^b(0) = \frac{1}{\sqrt{r}}(1, \cdots, 1)^T$ (see [15]). In fact if $\widehat{\Phi}(0) \in R^r$ is a vector with $\widehat{\Phi}(0)^T\widehat{\Phi}(0) = 1$, then there exists a $r \times r$ orthogonal matrix $\mathbf{U}$ such that $\mathbf{U}\widehat{\Phi}(0) = \frac{1}{\sqrt{r}}(1, \cdots, 1)^T$. Let $\{\mathbf{H}^b, \mathbf{G}^b\}$ be the multifilter bank defined by

$$\mathbf{H}^b = \mathbf{U}\mathbf{H}\mathbf{U}^T, \quad \mathbf{G}^b = \mathbf{U}_1\mathbf{G}\mathbf{U}^T,$$

where $\mathbf{U}_1$ is an orthogonal matrix. Then $\{\mathbf{H}^b, \mathbf{G}^b\}$ is orthogonal and generates the scaling function Φ^b and the multiwavelet Ψ^b with $\widehat{\Phi}^b(0) = \frac{1}{\sqrt{r}}(1, \cdots, 1)^T$, where $\Phi^b = \mathbf{U}\Phi, \Psi^b = \mathbf{U}_1\Psi$. As in [15], multiwavelet Ψ^b is said to be **balanced** if its corresponding scaling function Φ^b satisfies $\widehat{\Phi}^b(0) = \frac{1}{\sqrt{r}}(1, \cdots, 1)^T$. In this paper, we will use the second method and we will design the balanced multiwavelets.

Consider the case $r = 2$. From the decomposition algorithm (5) with multifilter bank $\{\mathbf{H}^b, \mathbf{G}^b\}$, the normalized lowpass frequency responses for this system are (see [19])

$$h^b_\alpha(\omega) := \sum_{k=0}^{N} \mathbf{H}^b_k(\alpha, 1)e^{-2ik\omega} + \mathbf{H}^b_k(\alpha, 2)e^{-i(2k+1)\omega}, \quad (8)$$

where $\alpha = 1, 2$; and for a matrix $\mathbf{B}$, $\mathbf{B}(\ell, j)$ denotes the (ℓ, j)-entry of $\mathbf{B}$. The filters h^b_1, h^b_2 act as lowpass filters. Thus it is required that $|h^b_\alpha(0)| = 1, h^b_\alpha(\pi) = 0, \alpha = 1, 2$. It was shown in [12] that if $\{\mathbf{H}^b, \mathbf{G}^b\}$ generates a balanced wavelet of multiplicity 2, then $h^b_\alpha(0) = 1, \alpha = 1, 2$. Thus in this case what in our design are the requirements:

$$h^b_1(\pi) \approx 0, \quad h^b_2(\pi) \approx 0. \quad (9)$$

B. Optimum time–frequency resolution multiwavelets

The design of OPTFR multiwavelets were studied in [11] and [12]. In this subsection, we review the procedure to design OPTFR multiwavelets.

The **time-duration** Δ_f of a window function f is defined by

$$\Delta_f := (\int_R (t - \bar{t})^2|f(t)|^2dt/E)^{\frac{1}{2}},$$

where

$$\bar{t} := \int_R t|f(t)|^2dt/E, \quad E := \int_R |f(t)|^2dt.$$

The **frequency-bandwidth** of f denoted by $\Delta_{\widehat{f}}$ is defined in the same way with f replaced by $\widehat{f}$. Then $\Delta_f\Delta_{\widehat{f}} \geq \frac{1}{2}$. This inequality is called the uncertainty principle, and the product $\Delta_f\Delta_{\widehat{f}}$ is called the **resolution cell**.

Since every component ψ_j of a multiwavelet Ψ is a bandpass function (see [11]), i.e., $\widehat{\psi}_j(0) = 0$, as in the scalar case, we also consider the frequency-bandwidth $\Delta^b_{\widehat{\psi}_j}$ of ψ_j defined by ([8], [6])

$$\Delta^b_{\widehat{\psi}_j} := (\int_0^{+\infty} (\omega - \bar{\bar{\omega}})^2|\widehat{\psi}_j(\omega)|^2d\omega \Big/ \int_0^{+\infty} |\widehat{\psi}_j(\omega)|^2d\omega)^{\frac{1}{2}},$$

where

$$\bar{\bar{\omega}} := \int_0^{+\infty} \omega|\widehat{\psi}_j(\omega)|^2d\omega \Big/ \int_0^{+\infty} |\widehat{\psi}_j(\omega)|^2d\omega.$$

In [11], formulas to compute the energy moments of scaling functions and multiwavelets in the time–frequency plane were provided. In the following we use $\Box_f$ and $\Box^b_f$ to denote $\Delta_f\Delta_{\widehat{f}}$ and $\Delta_f\Delta^b_{\widehat{f}}$, respectively.

To construct OPTFR multiwavelets, since the scaling functions and multiwavelets with good time–frequency localization are constructed simultaneously, the parametric expressions for the matrix coefficients $\mathbf{H}_k, \mathbf{G}_k$ of multifilter banks are required. In [12], several forms of factorizations for orthogonal causal FIR multifilter banks are provided based on the lattice structures for $M \times M$ FIR lossless systems. (About $M \times M$ FIR lossless systems, see, e.g., [20] and the references therein.) The factorization for orthogonal causal FIR multifilter banks which generate symmetric/antisymmetric scaling functions and multiwavelets is discussed in [13]. In the following we review the parametric expressions for the multifilter banks which generate wavelets of multiplicity 2 with symmetry property.

For a vector-valued function $\mathbf{f} = (f_1, f_2)^T$, we say $\mathbf{f}$ is symmetric/antisymmetric about a symmetry center $c_0 \in R$ if f_1 (f_2, respectively) is symmetric (antisymmetric, respectively) about the center c_0. Let $\{{}_N\mathbf{H}, {}_N\mathbf{G}\}$ with ${}_N\mathbf{H}(\omega) = \sum_{k=0}^N \mathbf{H}_k e^{-ik\omega}$, ${}_N\mathbf{G}(\omega) = \sum_{k=0}^N \mathbf{G}_k e^{-ik\omega}$ be an orthogonal FIR multifilter bank. If $\{{}_N\mathbf{H}, {}_N\mathbf{G}\}$ generates symmetric/antisymmetric scaling function ${}_N\Phi$ and multiwavelet ${}_N\Psi$ about the symmetry center $\frac{N}{2}$, then $\{\mathbf{H}_k\}_{k=0}^N, \{\mathbf{G}_k\}_{k=0}^N$ satisfy (see, e.g., [3]):

$$\mathbf{D}_0\mathbf{H}_{N-k}\mathbf{D}_0 = \mathbf{H}_k, \mathbf{D}_0\mathbf{G}_{N-k}\mathbf{D}_0 = \mathbf{G}_k, 0 \leq k \leq N, \quad (10)$$

where

$$\mathbf{D}_0 := \mathrm{diag}(1, -1).$$

If N is odd, $N = 2\gamma + 1$, $\gamma \in Z_+$ to say, then it was shown in [13] that $\{{}_{2\gamma+1}\mathbf{H}, {}_{2\gamma+1}\mathbf{G}\}$ is orthogonal and satisfies (10) if and only if

$$\begin{bmatrix} {}_{2\gamma+1}\mathbf{H}(\omega) \\ {}_{2\gamma+1}\mathbf{G}(\omega) \end{bmatrix} = \mathcal{M}_0\mathbf{V}_\gamma(z^2)\cdots\mathbf{V}_1(z^2)\mathcal{M}_0 \begin{bmatrix} {}_1\mathbf{H}(\omega) \\ {}_1\mathbf{G}(\omega) \end{bmatrix}, \quad (11)$$

where $z = e^{i\omega}$,

$$\mathbf{V}_k(z) := \frac{1}{2}\begin{bmatrix} \mathbf{I}_2 & \mathbf{v}_k \\ \mathbf{v}_k^T & \mathbf{I}_2 \end{bmatrix} + \frac{1}{2}\begin{bmatrix} \mathbf{I}_2 & -\mathbf{v}_k \\ -\mathbf{v}_k^T & \mathbf{I}_2 \end{bmatrix} z^{-1}, \quad (12)$$

with $\mathbf{v}_k \in O(2)$,

$$\begin{bmatrix} {}_1\mathbf{H}(\omega) \\ {}_1\mathbf{G}(\omega) \end{bmatrix} := \frac{1}{2} \begin{bmatrix} 1 & 0 \\ \cos\theta_0 & \mp\sin\theta_0 \\ 0 & \pm 1 \\ \sin\theta_0 & \pm\cos\theta_0 \end{bmatrix} + \frac{1}{2} \begin{bmatrix} 1 & 0 \\ -\cos\theta_0 & \mp\sin\theta_0 \\ 0 & \mp 1 \\ -\sin\theta_0 & \pm\cos\theta_0 \end{bmatrix} e^{-i\omega}, \tag{13}$$

with $-\pi < \theta_0 \le \pi$, and

$$\mathcal{M}_0 := \begin{bmatrix} 1 & 0 & 0 & 0 \\ 0 & 0 & 1 & 0 \\ 0 & 1 & 0 & 0 \\ 0 & 0 & 0 & 1 \end{bmatrix}.$$

Here $O(2)$ denotes the set consisting of all 2×2 orthogonal matrices. For $\mathbf{v}_k \in O(2)$, $0 \le k \le \gamma$, $\mathbf{v}_k$ are given by $\mathbf{v}_k = \mathbf{R}(\theta_k)\mathrm{diag}(1, \pm 1)$, $-\pi < \theta_k \le \pi$, where

$$\mathbf{R}(\theta_k) = \begin{bmatrix} \cos\theta_k & -\sin\theta_k \\ \sin\theta_k & \cos\theta_k \end{bmatrix}.$$

If $N = 2\gamma$ for some positive integer γ, a family of orthogonal multifilter banks $\{{}_{2\gamma}\mathbf{H}, {}_{2\gamma}\mathbf{G}\}$ which satisfy (10) are provided in [12]:

$$\begin{bmatrix} {}_{2\gamma}\mathbf{H}(\omega) \\ {}_{2\gamma}\mathbf{G}(\omega) \end{bmatrix} = \mathcal{M}_0 \mathbf{V}_{\gamma-1}(z^2)\mathbf{V}_{\gamma-2}(z^2)\cdots\mathbf{V}_1(z^2)\mathcal{M}_0 \begin{bmatrix} {}_2\mathbf{H}(\omega) \\ {}_2\mathbf{G}(\omega) \end{bmatrix}, \tag{14}$$

where $\mathbf{V}_k$ are given by (12) for some $\mathbf{v}_k \in O(2)$ and

$$\begin{bmatrix} {}_2\mathbf{H}(\omega) \\ {}_2\mathbf{G}(\omega) \end{bmatrix} = \frac{1}{4} \begin{bmatrix} 1 & -1 \\ -\sqrt{2}\cos\theta_0 & \sqrt{2}\cos\theta_0 \\ \pm 1 & \mp 1 \\ -\sqrt{2}\sin\theta_0 & \sqrt{2}\sin\theta_0 \end{bmatrix} + \frac{1}{2} \begin{bmatrix} 1 & 0 \\ 0 & \mp\sqrt{2}\sin\theta_0 \\ \mp 1 & 0 \\ 0 & \pm\sqrt{2}\cos\theta_0 \end{bmatrix} z^{-1} + \frac{1}{4} \begin{bmatrix} 1 & 1 \\ \sqrt{2}\cos\theta_0 & \sqrt{2}\cos\theta_0 \\ \pm 1 & \pm 1 \\ \sqrt{2}\sin\theta_0 & \sqrt{2}\sin\theta_0 \end{bmatrix} z^{-2} \tag{15}$$

with $-\pi < \theta_0 \le \pi, z = e^{i\omega}$.

The scaling functions ${}_N\Phi$ and multiwavelets ${}_N\Psi$ generated by $\{{}_N\mathbf{H}, {}_N\mathbf{G}\}$ which are given in (11) and (14) are symmetric/antisymmetric. Thus ${}_N\widehat{\Phi}(0) = (1, 0)^T$ and hence ${}_N\Psi$ is not balanced. By a rotation of the angle $\pi/4$, we get the balanced scaling function ${}_N\Phi^b$ and multiwavelet ${}_N\Psi^b$ by

$${}_N\Phi^b = \mathbf{R}_0\, {}_N\Phi, \quad {}_N\Psi^b = \mathbf{R}(\theta)\, {}_N\Psi, \tag{16}$$

where $\theta \in [-\pi, \pi)$ and

$$\mathbf{R}_0 := \mathbf{R}(\frac{\pi}{4}) = \frac{\sqrt{2}}{2} \begin{bmatrix} 1 & -1 \\ 1 & 1 \end{bmatrix}. \tag{17}$$

The problem is how to choose the number θ. In [15] and [19], θ is chosen to be 0, while in [12] θ is $\frac{\pi}{4}$. In our experiments about image compression, we find that for most cases we will get a little better results for the choice of $\theta = 0$ than for $\theta = \frac{\pi}{4}$. In the following, we set $\theta = 0$. In this case, the scale functions ${}_N\Phi^b = ({}_N\phi_1^b, {}_N\phi_2^b)^T$ satisfy ${}_N\phi_2^b(N - t) = {}_N\phi_1^b(t)$ and multiwavelets ${}_N\Psi = ({}_N\psi_1, {}_N\psi_2)^T$ are symmetric/antisymmetric. The corresponding multifilter banks, denoted by $\{{}_N\mathbf{H}^b, {}_N\mathbf{G}^b\}$, are given by

$${}_N\mathbf{H}^b(\omega) = \mathbf{R}_0\, {}_N\mathbf{H}(\omega)\mathbf{R}_0^T, \quad {}_N\mathbf{G}^b(\omega) = {}_N\mathbf{G}(\omega)\mathbf{R}_0^T. \tag{18}$$

It is shown in [12] that for $N = 2\gamma + 1$, the constrained conditions (9) for ${}_N\mathbf{H}^b$ are

$$\sin\theta_0 \approx 0. \tag{19}$$

while for $N = 2\gamma$, the constrained conditions (9) are

$$\cos(\theta_0 + \pi/4) \approx 0. \tag{20}$$

Using the parametric expression of $\{{}_N\mathbf{H}^b, {}_N\mathbf{G}^b\}$, we construct the balanced OPTFR multiwavelets by minimizing the objective function ${}_NS(1) := \Box_{{}_N\psi_1} + \Box_{{}_N\psi_2}$, or ${}_NS(2) := \Box^b_{{}_N\psi_1} + \Box^b_{{}_N\psi_2}$, or by minimizing the sum ${}_NS(3) := 2\Box_{{}_N\phi_1^b} + \Box_{{}_N\psi_1} + \Box_{{}_N\psi_2}$, or the sum ${}_NS(4) := 2\Box_{{}_N\phi_1^b} + \Box^b_{{}_N\psi_1} + \Box^b_{{}_N\psi_2}$ under condition (19) (for $N = 2\gamma + 1$) or (20) (for $N = 2\gamma$). In the first part of Section 4, we will determine which objective function we shall choose to construct OPTFR multiwavelets based on the image compression results. In [12], OPTFR balanced multiwavelets were constructed by minimizing $\Box_{{}_N\phi_1^b} + \Box_{{}_N\psi_1^b}$ and $\Box_{{}_N\phi_1^b} + \Box^b_{{}_N\psi_1^b}$, where ${}_N\Psi = \mathbf{R}_0\, {}_N\Psi$.

III. Nonexpansive symmetric extension transform

When we apply filter banks to image compression, we encounter the boundary conditions at the ends of the signals since in practice all signals are finite-length. In other words, we should extend the signal to the infinite interval. The extension approaches should satisfy the following conditions:

(1). Easy to implement. Due to the demand for time complexity, we can not design too complicated means to extend signals.

(2). Perfect reconstruction. If no error exists in the coding and quantization stages, the original signals can be perfectly reconstructed.

(3). Smoothness. No discontinuity is introduced by the extension process.

(4). Nonexpansive. That means no extra space overheads are imposed for the perfect reconstruction of the extended signals.

The most popular method for extension is the periodic extension. It works for any perfect reconstruction multirate filter bank. However, condition (3) can not be met anymore due to the differences between the first samples and the last samples of image signals.

Another extension approach is the symmetric extension. In comparison with the periodic extension, the symmetric extension improves the rate–distortion performance about 0.1–1.0dB in image compression. However its drawback is that it works only for the linear phase filters. As mentioned in the introduction, 2–channel orthogonal scalar wavelet filters can not be linear phases except for the trivial case (Haar system) [4]. So for 2–channel scalar wavelet orthogonal filters, periodic extension is the most used extension method for perfect reconstruction. Other method includes linear extrapolation of boundary samples [14].

Brislawn investigated the symmetric extension for the perfect reconstruction filter banks thoroughly [2]. A 2–channel orthogonal multifilter bank can be regarded as a 4–channel perfect reconstruction filter bank in some sense. However Brislawn's approach can not be applied or generalized directly to our multifilter banks which generate symmetric/antisymmetric multiwavelets. Strela *et al* have considered this issue for multifilter banks. But their method can only deal with the DGHM multifilter bank [18]. In this section we give our scheme for symmetric extension of the finite–length vector signals for the multifilter banks with the symmetric property. The finite–length vector signals $\mathbf{v}$ considered in this section are

$$\mathbf{v} = (\mathbf{v}_0, \mathbf{v}_1, \cdots, \mathbf{v}_{\ell-1}),$$

where ℓ is the length of the signal $\mathbf{v}$, and $\mathbf{v}_i = (v_{i,1}, v_{i,2})^T \in R^2$, $0 \le i \le \ell - 1$.

In the following we consider the symmetric extension transform for the matrix filters with a more general symmetry. Assume throughout that $\mathbf{S}$ is a 2×2 real matrix satisfying

$$\mathbf{S}^2 = \mathbf{I}_2, \quad \det(\mathbf{S}) = -1. \tag{21}$$

Clearly $\mathbf{D}_0$ is a matrix satisfying (21).

Definition 1 (**Symmetric multifilter**). A matrix filter $\mathbf{H}$ is said to be symmetric under $\mathbf{S}$ with the symmetric center $\frac{N}{2}$ for some integer N if

$$\mathbf{S}\mathbf{H}_{N-k}\mathbf{S} = \mathbf{H}_k, \quad k \in Z. \tag{22}$$

If a matrix filter $\mathbf{H}$ is symmetric (under $\mathbf{S}$) with the symmetric center $\frac{N}{2}$, then we denote it by $\mathrm{cen}(\mathbf{H}) = \frac{N}{2}$. For a matrix filter $\mathbf{H}(\omega) = \sum_{k=N_1}^{N_2} \mathbf{H}_k e^{-ik\omega}$ with $\mathbf{H}_k \neq \mathbf{0}$ for $k = N_1, N_2$, we use $\mathrm{len}(\mathbf{H}) := N_2 - N_1 + 1$ to denote the filter length of $\mathbf{H}$.

For 2–channel filter banks, the translations of filters with $2k, k \in Z$ do not affect the performance (see [2]). This property still holds for multifilter banks. So, without loss of the generality, we classify the symmetric matrix filters $\mathbf{H}$ into 4 types:

- Type I: $\mathrm{len}(\mathbf{H}) = 2N_1 + 1, N_1 \in Z$, and $\mathrm{cen}(\mathbf{H}) = 0$, i.e.

$$\mathbf{H}(\omega) = \sum_{k=-N_1}^{N_1} \mathbf{H}_k e^{-ik\omega}, \quad \mathbf{H}_k = \mathbf{S}\mathbf{H}_{-k}\mathbf{S};$$

- Type II: $\mathrm{len}(\mathbf{H}) = 2N_1 + 1, N_1 \in Z$, and $\mathrm{cen}(\mathbf{H}) = 1$, i.e.

$$\mathbf{H}(\omega) = \sum_{k=1-N_1}^{N_1+1} \mathbf{H}_k e^{-ik\omega}, \quad \mathbf{H}_k = \mathbf{S}\mathbf{H}_{2-k}\mathbf{S}.$$

- Type III: $\mathrm{len}(\mathbf{H}) = 2N_1, N_1 \in Z$, and $\mathrm{cen}(\mathbf{H}) = -\frac{1}{2}$, i.e.

$$\mathbf{H}(\omega) = \sum_{k=-N_1}^{N_1-1} \mathbf{H}_k e^{-ik\omega}, \quad \mathbf{H}_k = \mathbf{S}\mathbf{H}_{-1-k}\mathbf{S}.$$

- Type IV: $\mathrm{len}(\mathbf{H}) = 2N_1, N_1 \in Z$, and $\mathrm{cen}(\mathbf{H}) = \frac{1}{2}$, i.e.

$$\mathbf{H} = \sum_{k=1-N_1}^{N_1} \mathbf{H}_k e^{-ik\omega}, \quad \mathbf{H}_k = \mathbf{S}\mathbf{H}_{1-k}\mathbf{S}.$$

Definition 2 (**Symmetric signal**). For an infinite vector signal $\mathbf{v} = (\cdots, \mathbf{v}_{-1}, \mathbf{v}_0, \mathbf{v}_1, \mathbf{v}_2, \cdots)$, where $\mathbf{v}_k \in R^2, k \in Z$, if there exists an integer n such that $\mathbf{S}\mathbf{v}_{n-k} = \mathbf{v}_k, \forall k \in Z$, then we say that $\mathbf{v}$ is symmetric (under $\mathbf{S}$) with the symmetric center $\frac{n}{2}$. If $\mathbf{v}$ has two symmetric centers c_1 and c_2 with $c_1 < c_2$, we denote it by $\mathrm{cen}(\mathbf{v}) = (c_1, c_2)$.

Definition 3 (**Symmetric extension**). For a finite vector signal $\mathbf{v} = (\mathbf{v}_0, \mathbf{v}_1, \cdots, \mathbf{v}_m)$, an infinite signal $\mathbf{v}_{ext} = (\cdots, (\mathbf{v}_{ext})_{-1}, (\mathbf{v}_{ext})_0, (\mathbf{v}_{ext})_1, \cdots)$ is said to be the extension of $\mathbf{v}$, if $(\mathbf{v}_{ext})_k = \mathbf{v}_k, 0 \le k \le m$. If $\mathbf{v}_{ext}$ is symmetric with the symmetric centers c_1, c_2, i.e., $\mathrm{cen}(\mathbf{v}_{ext}) = (c_1, c_2)$, then $\mathbf{v}_{ext}$ is said to be the symmetric extension of $\mathbf{v}$ with the left symmetric center c_1 and the right symmetric center c_2. Let $\mathbf{v}_{ext}(c_1, c_2)$ denote $\mathbf{v}_{ext}$ to emphasize the symmetric centers of $\mathbf{v}_{ext}$.

As pointed out in [2], for subband coding, symmetric extensions of scalar signals can be reduced to two different types of extension depending on the parities of the lengths of the scalar filters considered. For the vector case, the extension of a vector signal also depends on the parities of the lengths of the matrix filters. However the vector signals are extended symmetrically in a slight different way. It depends also on the matrix $\mathbf{S}$ in (22).

Assume that the input finite–length vector signal is $(\mathbf{v}_0, \mathbf{v}_1, \cdots, \mathbf{v}_{\ell-1})$. For the even length matrix filters, the symmetric extension $\mathbf{v}_{ext}$ of $\mathbf{v}$ is given by

$$\begin{aligned}&\mathbf{v}_{ext}(-\frac{1}{2}, \ell - \frac{1}{2}) = \\ &(\cdots, \mathbf{S}\mathbf{v}_2, \mathbf{S}\mathbf{v}_1, \mathbf{S}\mathbf{v}_0, \mathbf{v}_0, \mathbf{v}_1, \cdots, \mathbf{v}_{\ell-1}, \mathbf{S}\mathbf{v}_{\ell-1}, \mathbf{S}\mathbf{v}_{\ell-2}, \cdots),\end{aligned} \tag{23}$$

while for the odd length matrix filters, the symmetric extension $\mathbf{v}_{ext}$ of $\mathbf{v}$ is given by

$$\begin{aligned}&\mathbf{v}_{ext}(0, \ell - 1) = \\ &(\cdots, \mathbf{S}\mathbf{v}_2, \mathbf{S}\mathbf{v}_1, \mathbf{v}_0, \mathbf{v}_1, \cdots, \mathbf{v}_{\ell-2}, \mathbf{v}_{\ell-1}, \mathbf{S}\mathbf{v}_{\ell-2}, \cdots).\end{aligned} \tag{24}$$

For the symmetric extension (24), it is required that the input signal satisfies

$$\mathbf{S}\mathbf{v}_0 = \mathbf{v}_0, \quad \mathbf{S}\mathbf{v}_{\ell-1} = \mathbf{v}_{\ell-1}. \tag{25}$$

The map from $\mathbf{v}$ to its symmetric extension $\mathbf{v}_{ext}$ defined by (23) or (24) is called the **symmetric extension transform**. We have the following two theorems about the symmetric extension transform.

Theorem 1: Suppose $\mathbf{H}$ is a matrix filter of Type I or Type II. Assume that the input signal $\mathbf{v}^{(0)} = (\mathbf{v}_0^{(0)}, \cdots, \mathbf{v}_{\ell-1}^{(0)})$ satisfies $\mathbf{S}\mathbf{v}_0^{(0)} = \mathbf{v}_0^{(0)}, \mathbf{S}\mathbf{v}_{\ell-1}^{(0)} = \mathbf{v}_{\ell-1}^{(0)}$. Let $\mathbf{v}_{ext}^{(0)}(0, \ell-1)$ be the symmetric extension of $\mathbf{v}^{(0)}$ defined by (24). Let $\mathbf{v}^{(-1)}$ be the output of subband filter $\mathbf{H}$: $\mathbf{v}_k^{(-1)} = \sqrt{2}\sum_n \mathbf{H}_{n-2k}(\mathbf{v}_{ext}^{(0)})_n$. Then $\mathbf{v}^{(-1)}$ is symmetric about 0 and $\frac{\ell-1}{2}$ if $\mathrm{cen}(\mathbf{H}) = 0$, and $\mathbf{v}^{(-1)}$ is symmetric about $-\frac{1}{2}$ and $\frac{\ell}{2} - 1$ if $\mathrm{cen}(\mathbf{H}) = 1$.

Proof: If $\mathrm{cen}(\mathbf{H}) = 0$, then $\mathbf{S}\mathbf{H}_{-i}\mathbf{S} = \mathbf{H}_i, i \in Z$. Thus

$$\begin{aligned}
\mathbf{v}_k^{(-1)} &= \sqrt{2}\sum_i \mathbf{H}_i \mathbf{v}_{2k+i}^{(0)} = \sqrt{2}\sum_i \mathbf{S}\mathbf{H}_{-i}\mathbf{S}\mathbf{v}_{2k+i}^{(0)} \\
&= \sqrt{2}\sum_i \mathbf{S}\mathbf{H}_i\mathbf{S}\mathbf{v}_{2k-i}^{(0)} \\
&= \sqrt{2}\mathbf{S}\sum_i \mathbf{H}_i \mathbf{v}_{-2k+i}^{(0)} = \mathbf{S}\mathbf{v}_{-k}^{(-1)},
\end{aligned}$$

and

$$\begin{aligned}
\mathbf{v}_k^{(-1)} &= \sqrt{2}\sum_i \mathbf{H}_i \mathbf{v}_{2k+i}^{(0)} = \sqrt{2}\mathbf{S}\sum_i \mathbf{H}_i\mathbf{S}\mathbf{v}_{2k-i}^{(0)} \\
&= \sqrt{2}\mathbf{S}\sum_i \mathbf{H}_i \mathbf{v}_{2\ell-2-2k+i}^{(0)} = \mathbf{S}\mathbf{v}_{\ell-1-k}^{(-1)}.
\end{aligned}$$

That is $\mathbf{v}^{(-1)}$ is symmetric about 0 and $\frac{\ell-1}{2}$.

For the case that $\mathrm{cen}(\mathbf{H}) = 1$, the symmetry of $\mathbf{v}^{(-1)}$ can be shown in a similar way, and the details are omitted here. ■

Theorem 2: Suppose $\mathbf{H}$ is a matrix filter of Type III or Type IV. Let $\mathbf{v}_{ext}^{(0)}(-\frac{1}{2}, \ell-\frac{1}{2})$ be the symmetric extension of $\mathbf{v}^{(0)}$ defined by (23) and $\mathbf{v}^{(-1)}$ be the output of subband filter $\mathbf{H}$: $\mathbf{v}_k^{(-1)} = \sqrt{2}\sum_n \mathbf{H}_{n-2k}(\mathbf{v}_{ext}^{(0)})_n$. Then $\mathbf{v}^{(-1)}$ is symmetric about 0 and $\frac{\ell}{2}$ if $\mathrm{cen}(\mathbf{H}) = -\frac{1}{2}$, and $\mathbf{v}^{(-1)}$ is symmetric about $-\frac{1}{2}$ and $\frac{\ell-1}{2}$ if $\mathrm{cen}(\mathbf{H}) = \frac{1}{2}$.

Theorem 2 can be established as Theorem 1, and here we would not provide the details.

For $c \in R$, let $[c]$ denotes the largest integer not greater than c. In the following, we define the storage length of a symmetric signal.

Definition 4 (**Storage length**). Suppose $\mathbf{v}(c_1, c_2)$ is an infinite signal with the left symmetric center c_1 and the right symmetric center c_2. Denote $\mathbf{v}^0 = (\mathbf{v}_{\ell_1}, \mathbf{v}_{\ell_1+1}, \mathbf{v}_{\ell_1+2}, \cdots, \mathbf{v}_{\ell_2})$, where $\ell_1 = [c_1 + \frac{1}{2}], \ell_2 = [c_2]$. Define $storl(\mathbf{v}_{\ell_1}) := \frac{1}{2}$ if c_1 is an integer and $storl(\mathbf{v}_{\ell_1}) := 1$ if c_1 is not an integer, and define $storl(\mathbf{v}_{\ell_2})$ in a similar way. Define $storl(\mathbf{v}^0) := \ell_2 - \ell_1 - 1 + storl(\mathbf{v}_{\ell_1}) + storl(\mathbf{v}_{\ell_2})$ and $storl(\mathbf{v}) := storl(\mathbf{v}^0)$.

Remark 1: In Definition 4, if the left center c_1 is an integer, i.e., $c_1 = \ell_1$ for some integer ℓ_1, then $\mathbf{v}_{\ell_1}$ satisfies $\mathbf{S}\mathbf{v}_{\ell_1} = \mathbf{v}_{\ell_1}$. Thus $\mathbf{v}_{\ell_1} = k\mathbf{v}_{\mathbf{S}}$, where k is a constant and $\mathbf{v}_{\mathbf{S}}$ is the normalized real right eigenvector of $\mathbf{S}$ corresponding to eigenvalue 1. Therefore one parameter k is enough to determine vector $\mathbf{v}_{\ell_1}$. Thus in this case, compared with other vectors $\mathbf{v}_j, \ell_1 < j < \ell_2$, half storage is needed to store $\mathbf{v}_{\ell_1}$; and we define $storl(\mathbf{v}_{\ell_1})$ to be $\frac{1}{2}$. For the same reason, if $c_2 = \ell_2$ for some integer ℓ_2, then we define $storl(\mathbf{v}_{\ell_2}) = \frac{1}{2}$. The number $storl(\mathbf{v})$ is the actual number we need to store the vector signal $\mathbf{v}$.

By a direct calculation, we have the following proposition.

Proposition 1: Let $\mathbf{v}(c_1, c_2)$ be an infinite vector signal with the left symmetric center c_1 and the right symmetric center c_2. Then $storl(\mathbf{v}) = c_2 - c_1$.

In the symmetric extension of a finite–length vector signal for the odd length matrix filter, (25) imposes an extra constraint on the original vector signal. However, most vector signals do not meet this condition automatically. To overcome this problem, we develop a transform to generate the input vector signal from the original scalar signal, and the vector signal derived can be used as the input signal for a matrix filter no matter the length of the matrix filter is odd or even.

If $\mathbf{S}$ is a matrix satisfying (21), then 1 and -1 are eigenvalues of $\mathbf{S}$. Thus there is a non–singular matrix $\mathbf{U}$ such that

$$\mathbf{U}^{-1}\mathbf{S}\mathbf{U} = \mathbf{D}_0.$$

Recall $\mathbf{D}_0 = \mathrm{diag}(1, -1)$. Let $\mathbf{R}_0$ be the matrix defined by (17). In the following we define the transform $T_{\mathbf{S}}$ associated with $\mathbf{S}$.

Transform $T_{\mathbf{S}}$. Suppose $f = (f_0, f_1, f_2, \cdots, f_{2\ell-1})$ is the sample of the original scalar signal.

(1) If the length of the matrix filter is even, define the vector signal $\mathbf{v} = (\mathbf{v}_0, \mathbf{v}_1, \mathbf{v}_2, \cdots, \mathbf{v}_{\ell-1})$ of length ℓ by

$$\mathbf{v}_i = \mathbf{U}\mathbf{R}_0^T \begin{pmatrix} f_{2i} \\ f_{2i-1} \end{pmatrix}, 0 \le i \le \ell - 1. \tag{26}$$

(2) If the length of the matrix filter is odd, define the vector signal $\mathbf{v} = (\mathbf{v}_0, \mathbf{v}_1, \mathbf{v}_2, \cdots, \mathbf{v}_{\ell-1}, \mathbf{v}_\ell)$ of length $\ell + 1$ by

$$\begin{cases} \mathbf{v}_0 = \mathbf{U}\mathbf{R}_0^T \binom{f_0}{f_0}, \mathbf{v}_\ell = \mathbf{U}\mathbf{R}_0^T \binom{f_{2\ell-1}}{f_{2\ell-1}}, \text{ and} \\ \mathbf{v}_i = \mathbf{U}\mathbf{R}_0^T \binom{f_{2i-1}}{f_{2i}}, \quad 1 \le i \le \ell - 1. \end{cases} \tag{27}$$

Let $T_{\mathbf{S}}$ denote the transform from the original scalar signal f to the vector signal $\mathbf{v}$, i.e., $T_{\mathbf{S}} f := \mathbf{v}$.

Proposition 2: Suppose $f = (f_0, f_1, \cdots, f_{2\ell-1})$ is the sample of the original signal. Let $T_{\mathbf{S}} f = (\mathbf{v}_0, \mathbf{v}_1, \mathbf{v}_2, \cdots, \mathbf{v}_{\ell-1}, \mathbf{v}_\ell)$ be the vector signal defined by (27), then $T_{\mathbf{S}} f$ satisfies (25).

Proof: Since $\mathbf{S}\mathbf{U} = \mathbf{U}\mathbf{D}_0$, one has

$$\begin{aligned}
\mathbf{S}\mathbf{v}_0 &= \mathbf{U}\mathbf{D}_0\mathbf{R}_0^T \begin{pmatrix} f_0 \\ f_0 \end{pmatrix} = \mathbf{U}\mathbf{D}_0 \begin{pmatrix} \sqrt{2} f_0 \\ 0 \end{pmatrix} \\
&= \mathbf{U}\mathbf{R}_0^T \begin{pmatrix} f_0 \\ f_0 \end{pmatrix} = \mathbf{v}_0.
\end{aligned}$$

Similarly we have $\mathbf{S}\mathbf{v}_\ell = \mathbf{v}_\ell$. ■

Proposition 2 ensures that the vector signal derived by transform $T_{\mathbf{S}}$ meets the requirement of the symmetric extension for the odd–length matrix filters. Since $\mathbf{U}\mathbf{R}_0^T$ is a linear operator, transform $T_{\mathbf{S}}$ preserves the continuity of the input signal.

Theorems 1, 2 and Proposition 1 lead to the following theorem.

Theorem 3: Suppose that $\{\mathbf{H}, \mathbf{G}\}$ is a multifilter bank, $\mathbf{H}$, $\mathbf{G}$ are symmetric under $\mathbf{S}$ and the lengths of $\mathbf{H}$, $\mathbf{G}$ have the same parity. For a scalar input signal $f = (f_0, f_1, \cdots, f_{2\ell-1})$, let $\mathbf{v}^{(0)} = T_{\mathbf{S}} f$ be the vector signal defined by (26) if the length of $\mathbf{H}$ is even and by (27) if the length of $\mathbf{H}$ is odd. Let $\mathbf{v}^{(0)}_{ext}$ be the symmetric extension of $\mathbf{v}^{(0)}$ defined (23) or (24) and $\mathbf{v}^{(-1)}, \mathbf{u}^{(-1)}$ be the the subband outputs of the input vector signal $\mathbf{v}^{(0)}_{ext}$ with multifilters $\mathbf{H}, \mathbf{G}$, respectively. Then

$$storl(\mathbf{v}^{(-1)}) + storl(\mathbf{u}^{(-1)}) = \ell. \tag{28}$$

Proof: First we consider the case that $\mathrm{len}(\mathbf{H})$ is even. In this case $\mathbf{v}^{(0)}_{ext}$ is the symmetric extension of $\mathbf{v}^{(0)}$ by (24). Theorem 2 shows that $\mathrm{cen}(\mathbf{v}^{(-1)}) = (0, \frac{\ell}{2})$ if $\mathbf{H}$ is of Type III, while $\mathrm{cen}(\mathbf{v}^{(-1)}) = (-\frac{1}{2}, \frac{\ell-1}{2})$ if $\mathbf{H}$ is of Type IV. Proposition 1 implies that for both cases,

$$storl(\mathbf{v}^{(-1)}) = \frac{\ell}{2}.$$

Since $\mathrm{len}(\mathbf{G})$ is also even, we also have $storl(\mathbf{u}^{(-1)}) = \frac{\ell}{2}$. Thus $storl(\mathbf{v}^{(-1)}) + storl(\mathbf{u}^{(-1)}) = \ell$. That is (28) holds true for the case that $\mathrm{len}(\mathbf{H})$ is even.

Now let us consider the case that $\mathrm{len}(\mathbf{H})$ is odd. Note that in this case, $\mathbf{v}^{(0)}_{ext}$ is the symmetric extension of $\mathbf{v}^{(0)} = (\mathbf{v}^{(0)}_0, \mathbf{v}^{(0)}_1, \cdots, \mathbf{v}^{(0)}_\ell)$ given by (23). Theorem 1 shows that $\mathrm{cen}(\mathbf{v}^{(-1)}) = (0, \frac{\ell}{2})$ if $\mathbf{H}$ is of Type I, while $\mathrm{cen}(\mathbf{v}^{(-1)}) = (-\frac{1}{2}, \frac{\ell}{2} - \frac{1}{2})$ if $\mathbf{H}$ is of Type II. From Proposition 1, for both cases,

$$storl(\mathbf{v}^{(-1)}) = \frac{\ell}{2}.$$

In the same way, one has $storl(\mathbf{u}^{(-1)}) = \frac{\ell}{2}$. Thus $storl(\mathbf{v}^{(-1)}) + storl(\mathbf{u}^{(-1)}) = \ell$. That is (28) holds for the case that $\mathrm{len}(\mathbf{H})$ is odd. ∎

Theorem 3 implies

Corollary 1: The symmetric extension transforms defined by (23) and (24) are nonexpansive.

In the following let us consider two special cases. If $\{\mathbf{H}, \mathbf{G}\}$ is an FIR multifilter bank generating symmetric/antisymmetric scaling functions and multiwavelets, then $\mathbf{H}, \mathbf{G}$ satisfy (22) with $\mathbf{S} = \mathbf{D}_0$. In this case, we can choose $\mathbf{U}$ to be $\mathbf{I}_2$. Thus the corresponding transform is given by (26) and (27) with $\mathbf{U} = \mathbf{I}_2$. By Corollary 1, for such a multifilter bank $\{\mathbf{H}, \mathbf{G}\}$, the symmetric extension transforms defined by (23) and (24) with $\mathbf{S} = \mathbf{D}_0$ are nonexpansive.

Assume that $\{\mathbf{H}, \mathbf{G}\}$ is an FIR multifilter bank. Let $\{\mathbf{H}^b, \mathbf{G}^b\}$ be the multifilter filter banks defined by

$$\mathbf{H}^b = \mathbf{R}_0 \mathbf{H} \mathbf{R}_0^T, \quad \mathbf{G}_1^b = \mathbf{R}_0 \mathbf{G} \mathbf{R}_0^T.$$

Then one can show that both $\mathbf{H}$ and $\mathbf{G}$ are symmetric under $\mathbf{D}_0$ if and only if $\mathbf{H}^b$ and $\mathbf{G}_1^b$ are symmetric under $\mathbf{E}$, where

$$\mathbf{E} := \begin{bmatrix} 0 & 1 \\ 1 & 0 \end{bmatrix}$$

is the exchange matrix. For $\mathbf{S} = \mathbf{E}$, choose $\mathbf{U} = \mathbf{R}_0$. Then $\mathbf{U}^{-1}\mathbf{E}\mathbf{U} = \mathbf{D}_0$. Thus in this case for the the original scalar signal $f = (f_0, f_1, f_2, \cdots, f_{2\ell-1})$, the corresponding transform, denoted by $\mathbf{T_E}$, is given by $\mathbf{T_E} f := \mathbf{v}$, where $\mathbf{v} = (\mathbf{v}_0, \mathbf{v}_1, \mathbf{v}_2, \cdots, \mathbf{v}_{\ell-1})$ with

$$\mathbf{v}_i = \begin{pmatrix} f_{2i} \\ f_{2i-1} \end{pmatrix}, \quad 0 \le i \le \ell - 1 \tag{29}$$

if the length of the matrix filter is even, and $\mathbf{v} = (\mathbf{v}_0, \mathbf{v}_1, \mathbf{v}_2, \cdots, \mathbf{v}_{\ell-1}, \mathbf{v}_\ell)$ with

$$\mathbf{v}_0 = \begin{pmatrix} f_0 \\ f_0 \end{pmatrix}, \mathbf{v}_l = \begin{pmatrix} f_{2\ell-1} \\ f_{2\ell-1} \end{pmatrix}, \mathbf{v}_i = \begin{pmatrix} f_{2i-1} \\ f_{2i} \end{pmatrix}, 1 \le i \le \ell - 1 \tag{30}$$

if the length of the matrix filter is odd. Therefore, when we use $\{\mathbf{H}^b, \mathbf{G}_1^b\}$ as the analysis and synthesis multifilter banks, we use the transform $T_{\mathbf{E}}$ and the symmetric extension transforms given by (23) or (24) with $\mathbf{S} = \mathbf{E}$. Corollary 1 shows again that the symmetric extension transform with matrix $\mathbf{E}$ is nonexpansive. The vector input from a scalar signal defined by (29) and (26) with $\mathbf{U} = \mathbf{I}_2$ were also used in [18] and [19], respectively.

IV. Optimal multifilter banks for image compression

A. Objective function and optimal multifilter banks

Let $\{{}_N\mathbf{H}^b, {}_N\mathbf{G}^b\}$ be the orthogonal FIR multifilter filter banks given by (18) with ${}_N\mathbf{H}$ and ${}_N\mathbf{G}$ given by (11) and (14), and $\pm$, $\mp$ in (13) and (15) being $+$ and $-$, respectively, and $\mathbf{v}_k \in O(2)$ in (12) being $\mathbf{R}(\theta_k)$. Let ${}_N\Phi^b, {}_N\Psi$ denote the scaling functions and multiwavelets generated by $\{{}_N\mathbf{H}^b, {}_N\mathbf{G}^b\}$. To construct OPTFR multiwavelets, we shall determine which objective function ${}_NS(j)$, $1 \le j \le 4$ we shall use. In the following the constrained conditions (19) and (20) used are respectively

$$\begin{cases} |\sin\theta_0| \le 10^{-4} (\text{ for } N = 2\gamma + 1), \\ |\cos(\theta_0 + \pi/4)| \le 10^{-4} (\text{ for } N = 2\gamma). \end{cases} \tag{31}$$

We consider the case $N = 9$. By minimizing different objective functions under (31), we obtain the corresponding parameters and hence the scaling functions Φ^b and multiwavelets Ψ. In Table 1, we provide the areas of the resolution cells of Φ^b and Ψ. All the resulting scaling functions Φ^b provide approximation order 1. (About the approximation order of functions, see [9].) Let $\mathrm{Ort}_{10}(j)$, denote the corresponding optimal multifilter banks obtained by minimizing ${}_NS(j), 1 \le j \le 4$. In Table 2, we list the compression results for 512×512 standard images Lena and Barbara using $\mathrm{Ort}_{10}(j), 1 \le j \le 4$ (see the implementation of $\mathrm{Ort}_{10}(j)$ for image compression in the next subsection).

From Tables 2, the performances in image compression of the optimal multifilter banks obtained by minimizing different objective functions are comparable. The optimal multifilter bank obtained with ${}_9S(4)$ has a little better performance. We also tested optimal multifilter banks of other lengths. We find in some cases and for the Barbara image, the optimal multifilter banks obtained by minimizing ${}_NS(3)$ also provide a good performance. However in general, the optimal multifilter banks by minimizing ${}_NS(4)$ provide a good and stable performance for both Lena image and Barbara image. The reasons might be that in the multiwavelet decomposition and reconstruction algorithms, the lowpass filters ${}_N\mathbf{H}^b$ are used as the highpass filters ${}_N\mathbf{G}^b$, and it plays the similar role as ${}_N\mathbf{G}^b$. Thus the scaling functions shall also have good time–frequency localization as multiwavelets. In the following we choose ${}_NS(4)$ as the objective function, and let Ort_{N+1} denote the corresponding optimal multifilter banks.

In Table 3, we provide some parameters for the optimal multifilter banks and the areas of the resolution cells of the corresponding OPTFR scaling functions (denoted by ${}_N\Phi^{bo} = ({}_N\phi_1^{bo}, {}_N\phi_2^{bo})^T$) and multiwavelets (denoted by ${}_N\Psi^o = ({}_N\psi_1^o, {}_N\psi_2^o)^T$). From Table 3, we find the scaling functions and multiwavelets with longer lengths have smaller areas of the resolution cells. By the parameters in Table 3 and the expressions of the multifilter banks, one can get the optimal multifilter banks. In Appendix, we provide Ort_{N+1} for $N = 3, 4, 5$.

B. Image compression

Let $\{{}_N\mathbf{H}^b, {}_N\mathbf{G}^b\}$ be the multifilter back given by (18). Since ${}_N\mathbf{G}^b$ does not satisfy the symmetric properties as ${}_N\mathbf{H}^b$ and we cannot use directly the symmetric extension transform provided in the above section, we first discuss the implementation of the symmetric extension transform for $\{{}_N\mathbf{H}^b, {}_N\mathbf{G}^b\}$. Define ${}_N\mathbf{G}_1^b := \mathbf{R}_0\, {}_N\mathbf{G}^b$. Then ${}_N\mathbf{H}^b, {}_N\mathbf{G}_1^b$ are symmetric under $\mathbf{E}$. Thus for scalar signals, we generate the vector signals $\mathbf{v}$ by the transform $T_\mathbf{E}$ defined by (29) and (30). Then we use the symmetric extension transform of $\mathbf{v}$ for $\{{}_N\mathbf{H}^b, {}_N\mathbf{G}_1^b\}$ provided in Section III to produce the symmetric vector signals and compute $\mathbf{v}^{(-J)}$ and $\mathbf{w}^{(-j)}, 1 \le j \le J$ with the discrete multiwavelet decomposition algorithm. Since ${}_N\mathbf{G}^b = \mathbf{R}_0^T\, {}_N\mathbf{G}_1^b$, the highpass outputs for $\{{}_N\mathbf{H}^b, {}_N\mathbf{G}^b\}$ are $\mathbf{R}^T\mathbf{w}^{(-j)}$. We develop an algorithm based on embedded zero-tree wavelet (EZW) (see [16]) with 5 level multiwavelet decomposition ($J = 5$) for further quantization and coding of $\mathbf{v}^{(-5)}$ and $\mathbf{R}^T\mathbf{w}^{(-j)}, 1 \le j \le 5$. The compression results for 512×512 standard images Lena and Barbara using different optimal multifilter banks are listed in Table 4.

In Table 4, Ort_4(vmd3) denotes the multifilter bank of length 4 with the corresponding scaling function ${}_3\Phi^b$ providing approximation order 3. The corresponding parameters are: $\theta_0 = -.025661167176, \theta_1 = .252680255142$. The areas of the resolution cells for ${}_3\Phi^b$ and the corresponding multiwavelet ${}_3\Psi$ are: $\square_{{}_3\phi_1^b} = .70136$, $\square^b_{{}_3\psi_1} = 1.51150$ and $\square^b_{{}_3\psi_2} = 1.58041$. ${}_3\Psi$ is the multiwavelet constructed in [3]. In Table 4, Ort_6(smth-v2) denotes the multifilter bank of length 6 with the corresponding scaling function ${}_5\Phi^b$ providing approximation order 2, ${}_5\Phi^b$ as smooth as possible and Ort_6(smth-v2) satisfying (9). The corresponding parameters are: $\theta_0 = .0001, \theta_1 = .459212307370, \theta_2 = -2.456942624174$. The scaling function ${}_5\Phi^b$ and the corresponding multiwavelet ${}_5\Psi$ are in $C^{1.27529}(R)$ (here we use the smoothness estimate provided in [10]). The areas of the resolution cells for ${}_5\Phi^b$ and ${}_5\Psi$ are: $\square_{{}_5\phi_1^b} = .67903$, $\square^b_{{}_5\psi_1} = 1.15052$ and $\square^b_{{}_5\psi_2} = 1.04253$. From Table 4, we find that good smoothness and approximation do not provide good multifilter banks for image compression.

In Tables 4, we also provide the image compression results with Daubechies' wavelet filter of length 8, denoted by D_8, Daubechies' least asymmetric wavelet filter of length 8, denoted by L_asym_8, and with the scalar $(9,7)$–tap biorthogonal wavelets filters, denoted by $S\_biort_{9,7}$. (See [1] and [4] about Daubechies' wavelet filters and $S\_biort_{9,7}$.) We find that for both Lena and Barbara images, the optimal multifilter banks Ort_N have better performances than D_8 and L_asym_8. For the Barbara image, Ort_N even have better performances than biorthogonal wavelet $S\_biort_{9,7}$, and for the Lena image, Ort_{16} has a better performance than $S\_biort_{9,7}$ for compression ratio (CR) 32 : 1. The original image of Barbara is shown in Fig. 1. The reconstructed images with compression ratio 32 : 1 by filter L_asym_8, $S\_biort_{9,7}$ and Ort_6 are shown in Fig. 2, Fig. 3 and Fig. 4, respectively. From Fig. 1–4, one can find that there is less distortion in texture parts of the image by the optimal multifilters than other scalar filters. See, for example, the scarf, trousers in Fig. 1–4. See also Fig. 5, Fig. 6, Fig. 7 and Fig. 8, the zooming in images of the right trousers in Fig. 1, Fig. 2, Fig. 3, and Fig. 4, respectively.

In Tables 4, we also provide the compression results using the periodic extension transform for some multifilter banks. From Tables 4, we conclude that the symmetric extension transform presented in Section 3 improves the rate–distortion performance, compared with the periodic extension transform.

Finally let us discuss the time complexity for the multiwavelet decomposition and reconstruction algorithms. For a scalar signal $\mathbf{v}$ of length L and a symmetric/antisymmetric matrix filter of length M, by the symmetric property of the matrix filter one can obtain that the time complexity for one level multiwavelet decomposition algorithm (5) and (6) and for the symmetric extension transform is LM multiplications and $L(2M-1)$ additions. The time complexity for the same length orthogonal scalar wavelet is about LM multiplications and $L(M-1)$ additions. In addition, the time complexity of the scalar $(9,7)$–tap biorthogonal wavelet filter is $4.5L$ multiplications and $7L$ additions, higher than those for the symmetric/antisymmetric matrix filter of length 4. Thus the time complexity for the multiwavelet decomposition and reconstruction algorithms and for our symmetric extension transform of the symmetric/antisymmetric matrix filters is very still low.

V. Conclusions

The design of optimal multifilter banks and optimum time–frequency resolution multiwavelets with different objective functions is discussed. The symmetric extension transform relate to multifilter banks with a more general symmetric property is presented. We show that the symmetric extension transforms are nonexpansive. The symmetric extension transforms for two kinds of special interesting multifilter banks, multifilter banks generate symmetric/antisymmetric multiwavelets and multifilter banks generate balanced multiwavelets, are discussed. More optimal multifilter banks for image compression are constructed and some of them are used in image compression. The experiments show that optimum time–frequency resolution multiwavelets have better performances in image compression than Daubechies' orthogonal wavelets and Daubechies' least asymmetric wavelets, and for some images, OPTFR multiwavelets even have better performances than the scalar $(9,7)$–tap biorthogonal wavelets. The experiments also show that the symmetric extension transform presented in this paper improves the rate–distortion performance, compared with the periodic extension transform.

Appendix

Denote $\mathbf{J} := \begin{bmatrix} 0 & -1 \\ 1 & 0 \end{bmatrix}$. The optimal multifilter banks $\mathrm{Ort}_{N+1} = \{{}_N\mathbf{H}^b, {}_N\mathbf{G}^b\}$ are given by ${}_N\mathbf{H}^b(\omega) = \mathbf{R}_0 {}_N\mathbf{H}(\omega)\mathbf{R}_0^T, {}_N\mathbf{G}^b(\omega) = {}_N\mathbf{G}(\omega)\mathbf{R}_0^T$, where $\mathbf{R}_0$ is defined by (17). In the following, we provide ${}_N\mathbf{H}, {}_N\mathbf{G}$ with $N = 3, 4, 5$.

For $N = 3$:

$$\mathbf{H}_0 = \begin{bmatrix} .008533247511 & .064759612742 \\ .008526771507 & -.064760465743 \end{bmatrix},$$

$$\mathbf{H}_1 = \begin{bmatrix} .491466752489 & .064759612742 \\ -.491473225993 & .064710465743 \end{bmatrix},$$

and $\mathbf{H}_j = \mathbf{D}_0\mathbf{H}_{3-j}\mathbf{D}_0$, $2 \le j \le 3$, $\mathbf{G}_k = (-1)^{k+1}\mathbf{H}_k\mathbf{J}, 0 \le k \le 3$.

For $N = 4$:

$$\mathbf{H}_0 = \begin{bmatrix} -.031578613037 & .031578613037 \\ -.042947457421 & .042947457421 \end{bmatrix},$$

$$\mathbf{H}_1 = \begin{bmatrix} .25 & -.164111400451 \\ .313173635648 & -.250024998750 \end{bmatrix},$$

$$\mathbf{H}_2 = \begin{bmatrix} .563157226074 & 0 \\ 0 & .414055082657 \end{bmatrix},$$

$$\mathbf{G}_0 = \begin{bmatrix} .042944299775 & -.042944299775 \\ .031574318449 & -.031574318449 \end{bmatrix},$$

$$\mathbf{G}_1 = \begin{bmatrix} -.25 & .313157226074 \\ -.164080083907 & .249974998750 \end{bmatrix},$$

$$\mathbf{G}_2 = \begin{bmatrix} .414111400451 & 0 \\ 0 & .563198634398 \end{bmatrix},$$

and $\mathbf{H}_j = \mathbf{D}_0\mathbf{H}_{4-j}\mathbf{D}_0$, $\mathbf{G}_j = \mathbf{D}_0\mathbf{G}_{4-j}\mathbf{D}_0$, $3 \le j \le 4$.

For $N = 5$:

$$\mathbf{H}_0 = \begin{bmatrix} -.015579570720 & .006797482939 \\ -.015580250391 & -.006795924948 \end{bmatrix},$$

$$\mathbf{H}_1 = \begin{bmatrix} .022474129485333 & -.051509844576 \\ -.022468978389 & -.051512091732 \end{bmatrix},$$

$$\mathbf{H}_2 = \begin{bmatrix} .493105441235 & -.058307327515 \\ .493111269502 & .058258016680 \end{bmatrix},$$

and $\mathbf{H}_j = \mathbf{D}_0\mathbf{H}_{5-j}\mathbf{D}_0$, $3 \le j \le 5$, $\mathbf{G}_k = (-1)^{k+1}\mathbf{H}_k\mathbf{J}, 0 \le k \le 5$.

Acknowledgment

The authors would like to thank the anonymous reviewers for helpful suggestions and comments on this paper.

References

[1] M. Antonini, M. Barlaud, P. Mathieu, and I. Daubechies, "Image coding using wavelet transform," *IEEE Trans. Image Processing*, vol. 1, pp. 205–220, 1992.
[2] C. M. Brislawn, "Classification of nonexpansive symmetric extension transform for multirate filter banks," *Applied and Computational Harmonic Analysis*, vol. 3, pp. 337–357, 1996.
[3] C. K. Chui and J. Lian, "A study on orthonormal multi-wavelets," *J. Appl. Numer. Math.*, vol. 20, pp. 273–298, 1996.
[4] I. Daubechies, *Ten Lectures on Wavelets.* CBMS-NSF Series in Appl. Math., vol. 61, Soc. Indus. Appl. Math. Publ., Philadelphia, PA, 1992.
[5] G. Donovan, J. Geronimo, D. Hardin and P. Massopust, "Construction of orthogonal wavelets using fractal interpolation functions," *Soc. Indus. Appl. Math. J. Math. Anal.*, vol. 27, pp. 1158–1192, 1996.
[6] C. Dorize and L. F. Villemoes, "Optimizing time-frequency resolution of orthonormal wavelets," in *Proc. IEEE. Int. Conf. Acoust., Speech, Signal Processing*, 1991, pp. 2029–2032.
[7] J. Geronimo, D. Hardin and P. Massopust, "Fractal functions and wavelet expansions based on several scaling functions," *J. Approx. Theory*, vol. 78, pp. 373–401, 1994.
[8] R. A. Haddad, A. N. Akansu and A Benyassine, "Time-frequency localization in transforms, subbands, and wavelet: A critical review," *Opt. Eng.*, vol. 32, pp. 1411–1429, July 1993.
[9] R. Q. Jia, "Refinable shift-invariant spaces:from splines to wavelets," in *Approximation Theory VIII*, vol. 2 (C. K. Chui and L. L. Schumaker, eds.), 1995, pp. 179–208.
[10] Q. Jiang, "On the regularity of matrix refinable functions," *Soc. Indus. Appl. Math. J. Math. Anal.* , vol. 29, pp. 1157–1176, 1998.
[11] ——, "Orthogonal multiwavelets with optimum time–frequency resolution," *IEEE Trans. Signal Processing*, vol. 46, pp. 830–844, Apr. 1998.
[12] ——, "On the design of multifilter banks and orthonormal multiwavelet bases," *IEEE Trans. Signal Processing*, vol. 46, pp. 3292–3303, Dec. 1998.
[13] ——, "Parameterization of M–channel orthogonal multifilter banks," preprint, 1997.
[14] G. Karlsson and M. Vetterli, "Extension of finite length signals for sub-band coding," *Signal Processing*, vol. 17, pp. 161–168, 1989.
[15] J. Lebrun and M. Vetterli, "Balanced multiwavelets theory and design," *IEEE Trans. Signal Processing*, vol. 46, pp. 1119–1125, Apr. 1998.
[16] J. M. Shapiro, "Embedded image coding using zerotree of wavelet coefficients," *IEEE Trans. Signal Processing*, vol. 41, pp. 3445–3462, Dec. 1993.
[17] G. Strang and T. Nguyen, *Wavelets and Filter Banks.* Wellesley, MA: Wellesley-Cambridge, 1996.
[18] V. Strela, P. Heller, G. Strang, P. Topiwala and C. Heil, "The application of multiwavelet filter banks to image processing," *IEEE Trans. Image Processing*, to be published.
[19] Y. Tham, L. Shen, S. L. Lee and H. H. Tan, "A general approach for analysis and application of discrete multiwavelet transform," *preprint*, 1997.
[20] P. P. Vaidyanathan, *Multirate Systems and Filter Banks*, Englewood Cliffs, NJ: Prentice Hall, 1993.
[21] X-G. Xia, "A new prefilter design for discrete multiwavelet transforms ," preprint, 1996.
[22] X-G. Xia, D. Hardin, J. Geronimo and B. Suter, "Design of prefilters for discrete multiwavelet transforms," *IEEE Trans. Signal Processing*, vol. 44, pp. 25–35, Jan. 1996.

Objective	$\square_{{}_9\phi_1^b}$	$\square_{{}_9\psi_1}$	$\square_{{}_9\psi_2}$	$\square^b_{{}_9\psi_1}$	$\square^b_{{}_9\psi_2}$
${}_9S(1)$	.66557	3.07060	3.45151		
${}_9S(2)$	.66942			1.02006	.82241
${}_9S(3)$	.66293	3.06795	3.45695		
${}_9S(4)$	.66746			1.01963	.82467

TABLE 1. The areas of the resolution cells of the OPTFR scaling functions and multiwavelets by different objective functions.

Filter	Lena			Barbara		
	32:1	64:1	100:1	16:1	32:1	64:1
$\mathrm{Ort}_{10}(1)$	34.063	31.016	29.360	31.208	27.435	25.676
$\mathrm{Ort}_{10}(2)$	34.077	31.020	29.369	31.253	27.437	25.686
$\mathrm{Ort}_{10}(3)$	34.046	31.013	29.363	31.214	27.429	25.680
$\mathrm{Ort}_{10}(4)$	*34.084*	*31.026*	*29.372*	*31.257*	*27.448*	*25.692*

TABLE 2. Compression results for different optimal multifilter banks derived by different objective functions.

Tao Xia was born in Gansu, China, on December 20, 1970. He received the B.S., M.S. and the Ph.D. degrees from Peking University, Beijing, China, in 1991, 1994 and 1997, respectively, all in applied mathematics. He is an NSTB post-doctoral fellow at the National University of Singapore from August 1997. His current research interests are wavelet application, pattern recognition and computer vision.

Qingtang Jiang was born in Zhejiang, China, on September 21, 1965. He received the B.S. and M.S. degrees from Hangzhou University, Hangzhou, China, in 1986 and 1989, respectively, and the Ph.D. degree from Peking University, Beijing, China, in 1992, all in mathematics. He was with Peking University, Beijing, China from July 1992 to August 1995. He was an NSTB post-doctoral fellow at the National University of Singapore from September 1995 to August 1997, and he is now a research fellow there. His current research interests are time-frequency analysis, wavelet theory and its applications, multifilter bank designs and signal classification.

Fig. 1. Original Barbara image.

Fig. 2. Reconstructed image using L_asym_8, compression ratio=32 : 1, PSNR=26.444dB.

Fig. 3. Reconstructed image using $S\_biort_{9,7}$, compression ratio=32 : 1, PSNR=26.738dB.

Fig. 4. Reconstructed image using optimal multifilter bank Ort_6, compression ratio=32 : 1, PSNR=27.488dB.

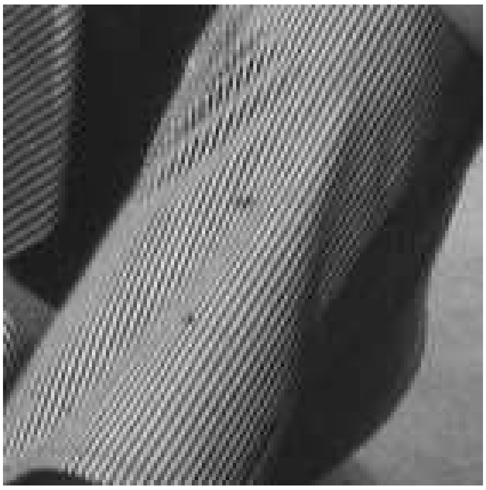

Fig. 5. A zooming in part of Fig. 1.

Fig. 6. A zooming in part of Fig. 2.

Fig. 7. A zooming in part of Fig. 3.

Fig. 8. A zooming in part of Fig. 4.

N	θ_0/θ_4	θ_1/θ_5	θ_2/θ_6	θ_3/θ_7	$\square_{N\phi_1^{bo}}$	$\square^b_{N\psi_1^o}$	$\square^b_{N\psi_2^o}$
3	.0001	.261926540380			.67576	1.25556	1.19626
4	.785498163398	2.838799865083			.68524	1.29019	1.23735
5	..0001	.587320842748	-2.318874548904		.69372	1.07752	.90340
6	-2.356294490193	-.798110754670	2.580483297003		.71321	1.16062	1.04136
7	3.141492653590	2.881761219789	-2.690949062435	.415045976633	.66821	1.03470	.84620
8	.785498163398	.273839049271	-2.824701076199	2.816782968532	.68166	1.05012	.87351
9	3.141492653590	-2.726999719581	.169573490290	1.693031112209	.66746	1.01963	.82467
	-1.526677145135						
11	.0001	1.563683228715	-1.626880780781	.233293866030	.67908	.98271	.75431
	1.175553687028	-1.928629589939					
13	.0001	1.494520214546	-1.946989428993	.407727304898	.70022	.87458	.61632
	-2.200455533167	-2.730009960499	.513113220909				
15	.0001	.084486838817	-.680782317254	2.179624036642	.77111	.84374	.60237
	-2.970957854756	.450131447798	-.320017962926	3.088460965915			

TABLE 3. The parameters for the optimal multifilter banks and the areas of the resolution cells of the corresponding OPTFR scaling functions and multiwavelets.

Filter		Lena			Barbara		
		32:1	64:1	100:1	16:1	32:1	64:1
Ort_4	Sym.	33.978	30.945	29.288	31.066	27.410	25.650
	Per.	33.702	30.734	28.924	30.812	27.107	25.588
Ort_4 (vmd3)	Sym.	33.903	30.902	29.219	30.886	27.241	25.592
	Per.	33.660	30.671	28.904	30.633	27.010	25.479
Ort_5	Sym.	34.000	30.973	29.205	31.068	27.279	25.622
	Per.	33.240	30.226	28.324	30.851	27.028	25.499
Ort_6	Sym.	33.814	30.864	29.256	31.037	27.488	25.638
	Per.	33.644	30.651	28.908	30.785	27.165	25.600
Ort_6 (smth-v2)	Sym.	33.783	30.838	29.236	30.933	27.407	25.612
	Per.	33.601	30.634	28.896	30.705	27.110	25.583
Ort_7	Sym.	33.887	30.921	29.315	31.163	27.693	25.678
	Per.	32.871	29.964	28.198	30.291	26.615	25.002
Ort_8		34.028	30.989	29.347	31.198	27.463	25.685
Ort_{16}		34.114	31.099	29.473	31.627	27.999	25.791
D_8		33.086	30.051	28.355	30.174	26.277	24.674
L_asym_8		33.409	30.405	28.894	30.295	26.444	24.988
$S\_biort_{9,7}$		34.108	31.154	29.789	30.827	26.738	25.206

TABLE 4. Compression results for images 'Lena' and 'Barbara' with multifilter banks (symmetric extension and periodic extension) and scalar wavelet filters D_8, L_asym_8 and $S\_biorth_{9,7}$.